PAPER

A novel HIF-1α/VMP1-autophagic pathway induces resistance to photodynamic therapy in colon cancer cells

M. E. Rodríguez, [ID] [a,b] C. Catrinacio, [ID] [b] A. Ropolo, [ID] [b] V. A. Rivarola [ID] [a] and M. I. Vaccaro [ID] *[b]

Colon cancer is the third most frequent cancer and the fourth most common cause of cancer-related mortality worldwide and the standard therapy is surgical resection plus adjuvant chemotherapy. Photodynamic therapy (PDT) has been proposed as an adjuvant therapy because it can prevent the tumor recurrence after surgical excision in colon cancer patients. Hypoxia is a common feature in solid tumors and leads to chemo/radioresistance. Recently, it has been shown that in response to hypoxia, cells can induce HIF-1α-mediated autophagy to survive in this hostile microenvironment. Moreover, hypoxia and autophagy have been implicated in the resistance to antitumor PDT. However, the molecular signals by which HIF-1α induces autophagy in the PDT context have not been studied yet. Here we evaluate the interplay between HIF-1α and autophagy as well as the underlying mechanism in the PDT resistance of colon cancer cells. Our study demonstrates that HIF-1α stabilization significantly increases VMP1-related autophagy through binding to hypoxia responsive elements in the VMP1 promoter. We show that HIF-1α-induced autophagy increases colon cancer cell survival as well as decreases cell death after PDT. Moreover, here we demonstrate that HIF-1α-induced autophagy is mediated by VMP1 expression, since the downregulation of VMP1 by the RNA interference strategy reduces HIF-1α-induced autophagy and cell survival after PDT. In conclusion, PDT induces autophagy as a survival mechanism and the induction of the novel HIF-1α/VMP1-autophagic pathway may explain, at least in part, the resistance of colon cancer cells to PDT. The knowledge of the molecular mechanisms involved in PDT resistance may lead to more accurate therapeutic strategies.

Introduction

Colon cancer is the third most frequent cancer and the fourth most common cause of cancer-related mortality worldwide, and the standard curative therapy is surgical resection plus adjuvant chemotherapy.[1,2] Effective treatment modalities are rare in cases of patients with peritoneal carcinomatosis and chemotherapy-resistant tumors.[3] Therefore, novel treatment modalities for such cases are required.

Photodynamic therapy (PDT) is an anti-tumor strategy that is approved for clinical use in a number of countries, for removing early-stage malignancies and palliation of symptoms in patients with late-stage tumors.[4,5] PDT involves the use of a light-sensitizing agent, or a photosensitizer, followed by illumination of the tumor with visible light; this leads to the production of reactive oxygen species (ROS) that cause direct damage to the tumor as well as the blood vessels supporting the tumor.[6] PDT is a promising anticancer treatment and its major pharmacological effect is to induce cancer cell apoptosis or necrosis through oxidative stress.[7]

PDT has been proposed as an adjuvant therapy because it can prevent the tumor recurrence after surgical excision in colon cancer patients.[8] In this sense, PDT may be most suitable for the treatment of small tumors or small areas of persistent tumors.[9] However, the prognosis is poor, particularly for patients with advanced stage tumors, due to their resistance to cell death, in which the hypoxic microenvironment potentially plays a critical role.[10] Solid tumors are subjected to hypoxia because they can quickly outgrow the existing vasculature and have decreased access to blood borne nutrients and O_2.[11,12] In this context, Hypoxia Inducible Factor-1 (HIF-1) is the major regulator of resistance to cell death and proliferation

[a]*Universidad Nacional de Río Cuarto, Departamento de Biología Molecular. Río Cuarto (5800), Córdoba, Argentina*
[b]*Universidad de Buenos Aires. CONICET. Facultad de Farmacia y Bioquímica. Instituto de Bioquímica y Medicina Molecular (IBIMOL), Buenos Aires, Argentina. E-mail: mvaccaro@ffyb.uba.ar*

This journal is © The Royal Society of Chemistry and Owner Societies 2017

Photochem. Photobiol. Sci., 2017, **16**, 1631–1642 | **1631**

of cancer cells by providing a growth advantage under hypoxic stress.[13]

Autophagy is defined as a process of programmed cell survival involving the sequestration of cellular components in double membrane structures called autophagosomes, which are degraded after fusion with lysosomes.[14] Autophagy increases cell survival and chemoresistance in different tumor cells.[15–17] Recently, it has been shown that in response to hypoxia, tumor cells may induce HIF-1-mediated autophagy to survive in that hostile microenvironment.[18,19] Thus, autophagy optimizes nutrient utilization in fast growing cells in response to hypoxia or metabolic stress contributing to cancer cell survival.[19] Hypoxia and autophagy promote resistance to PDT possibly through apoptosis inhibition in esophageal tumor cells.[20,21] Moreover, the inhibition of autophagy induces cell death by potentiating PDT-induced apoptosis in colorectal cancer stem-like cells.[22] However, the interplay between hypoxia and autophagy in the PDT context has not been studied yet.

Vacuole Membrane Protein 1 (VMP1) induces autophagy and plays an essential role in autophagosome formation in mammalian cells.[23–26] VMP1 also mediates a selective type of autophagy in the pancreas with acute pancreatitis, called zymophagy.[27] Moreover, oncogenic KRAS requires VMP1 expression to induce autophagy[28] and human pancreatic tumor cells activate VMP1-mediated autophagy in the presence of chemotherapy agents such as gemcitabine.[29]

Here we examine how HIF-1α and autophagy work together to modulate the cancer cell response to PDT and the molecular pathways by which HIF-1α induces autophagy to mediate PDT resistance in colon cancer cells. We found that PDT induces autophagy as a survival mechanism in colon cancer cells. We found that HIF-1α stabilization induces a novel HIF-1α/VMP1-autophagic pathway, which in turn, confers resistance to PDT.

Experimental

Cell culture

Human colon cancer CaCo2 cells (ATCC® HTB-37™) and SW480 (ATCC® CCL-228™) cells were cultured in Dulbecco's modified Eagle's medium (Sigma) supplemented with 10% fetal bovine serum (Internegocios), 100 U ml^{-1} penicillin, and 100 μg ml^{-1} streptomycin (Sigma) at 37 °C under a humidified atmosphere with 5% CO_2. Cells were transfected using the FuGENE-6 Transfection Reagent (Promega) as indicated by the manufacturer. For $CoCl_2$ treatment, CaCo2 and SW480 cells (10 × 10^4 cells per ml) were plated in 60 mm dishes. After 24 h the medium was replaced with complete medium with $CoCl_2$ (100, 200 or 400 μM) followed by a 24 h incubation. Cells were treated with 100 nM rapamycin, 5 mM 3-methyladenine (3-MA), 100 nM wortmannin (WM) or 10 μM chloroquine (CQ) when indicated. Cell viability was measured by using the 3-(4,5-dimethylthiazol-2-yl)-2,5-diphenyltetrazoliumbromide (MTT) assay.

Chemicals and the photosensitizer

The compound methyl derivative of δ-aminolevulinic acid (Sigma-Aldrich) as a precursor of the photosensitizer protoporphyrin IX (PpIX) was used in this work. A stock solution of 100 mM 5-aminolevulinic acid methyl ester (Me-ALA) was prepared in sterile PBS, from which 1 mM work solution was prepared employing DMEM culture medium without serum. Cobalt chloride ($CoCl_2$), rapamycin, 3-MA, WM, CQ, polyethylenimine (PEI), and Earle's Balanced Salt Solution (EBSS) were purchased from Sigma-Aldrich. Hoechst 33342 was purchased from Cell Signaling. All other reagents were of the highest analytical grade available.

Antibodies

The primary antibodies employed were: HIF-1α (R&D), microtubule-associated protein 1A/1B-light chain 3B (LC3B) (Cell Signaling), p62/SQSTM1 (Cell Signaling), VMP1AtgD (was developed in our laboratory),[23] β-actin (Sigma) and β-tubulin (Sigma). The secondary antibodies used were: horseradish peroxidase (HRP) monoclonal antibody anti-mouse IgG (Cell Signaling), HRP monoclonal antibody anti-rabbit IgG (Cell Signaling), polyclonal goat anti-rabbit IgG (H + L) secondary antibody Alexa Fluor® 594 conjugate (Thermo Scientific™), and IRDye® 680LT goat anti-rabbit IgG (H + L) (Licor).

Plasmids

5HRE-hCMV-d2EGFP (provided by T. Foster, University of Rochester, Rochester, NY), pRFP-LC3, pLKO.1-shRNAHIF-1α-1 (provided by Dr Eric Metzen, University of Duisburg-Essen, Essen, Germany), and pCMS3-H1p-EGFP that contains a VMP1 short hairpin RNA construction with the target sequence of VMP1-siRNA developed in our lab.[27]

Chromatin immunoprecipitation (ChIP) assay

Chromatin immunoprecipitation was conducted following the ChIP kit protocol (Pierce Agarose, Thermo Scientific). Briefly, CaCo2 cells (3 × 10^6) were cross-linked with 1% formaldehyde directly into the media for 10 min at room temperature. The cells were washed and scraped with phosphate-buffered saline and collected by centrifugation at 800g for 5 min at 4 °C, suspended in cell lysis buffer and incubated on ice for 15 min. The pellet was suspended in nuclear lysis buffer and sheared to fragment DNA to 700 bp. Samples were immunoprecipitated using a HIF-1α antibody (R&D), or a normal rabbit IgG antibody (Pierce Agarose, Thermo Scientific) overnight at 4 °C on a rotating wheel. Following immunoprecipitation, samples were washed and eluted using the chromatin immunoprecipitation kit in accordance with the manufacturer's instructions. Cross-links were removed at 62 °C for 1.5 h, and immunoprecipitated DNA was purified (Pierce Agarose ChIP Kit, Thermo Scientific) and subsequently amplified by PCR. PCR was performed using three primer sets for the three areas containing potential HIF-1α binding sites in the VMP1 promoter sequence (Fig. 2D): (1) ACCCAGTGAGACCTCATCTTT (sense) and CACTCCATTGAG ATATGGGACA (antisense); (2) GCCCGCACTAAGAGCCTAAC

1632 | *Photochem. Photobiol. Sci.*, 2017, **16**, 1631–1642

This journal is © The Royal Society of Chemistry and Owner Societies 2017

(sense) and CCCCAATTCCCTGAGTTAGTT (antisense); (3) GAGCCCTTGGAGAGGAACTT (sense) and CATGGAGTTGCA GGTAAATAAAAG (antisense). PCR products were visualized by using 1.5% agarose gel.

Band images were quantified digitally, using ImageJ software, and data were expressed as relative to the input expression (% of input).

HRE-EGFP reporter assay

HIF-1 transcriptional activity was assessed using a promoter–reporter plasmid 5HRE-hCMV-d2EGFP containing five tandem hypoxia response element (HRE) consensus sequences and a human CMV minimal promoter upstream of an enhanced GFP (EGFP) reporter gene that has been previously described by Vordermak and co-workers.[30] CaCo2 cells were transfected employing PEI as the transfection reagent, mixing 40 µl of cold 150 mM ClNa, 1 µg of DNA and finally adding 1 µl of PEI (1 µg µl^{-1}). This mixture was incubated at 37 °C for 15 min and then aggregated in the wells, where the cells were grown in 500 µl of complete medium. After 24 h the transfection medium was replaced with complete medium containing 200 µM CoCl$_2$. The EGFP expression was analyzed 24 h after treatment by using a confocal fluorescence microscope (FV1000; Olympus).

Immunoblotting

Cells were lysed and proteins were collected with RIPA buffer (150 mM NaCl, 1% Triton X-100, 1% sodium deoxycholate, 0.1% SDS, 10 mM Tris-HCl pH 7.2, 5 mM EDTA, and phosphatase and protease inhibitor cocktail [Sigma-Aldrich]). Protein concentration was determined using the bicinchoninic acid (BCA) protein assay reagent (Pierce). An equal amount of protein was analyzed on SDS-PAGE and transferred to polyvinylidene fluoride membranes (0.22 µm, Millipore). Membranes were first incubated at room temperature for 1 h in blocking buffer (5% low-fat milk powder in phosphate-buffered saline (PBS)), and then incubated overnight at 4 °C with primary antibodies. The horseradish peroxidase-conjugated secondary antibody was incubated for 2 h at room temperature. The detection of immunoreactive bands was carried out using the enhanced-chemoluminescence kit (GE Healthcare) according to the manufacturer's instructions. When indicated, IRDye secondary antibodies were used and revealed using Odyssey® SA (Licor). We used ImageJ software to quantify western blot bands. Relative densitometry is expressed as the mean ± SD of 5 different experiments. t test: *$P < 0.05$, **$P < 0.01$, ***$P < 0.001$.

Fluorescence microscopy

For immunofluorescence, after the treatment, cells growing on glass slides were fixed with cold methanol and nonspecific binding was blocked with 3% bovine serum albumin (BSA) in PBS (1% Tween 20). After overnight blocking, the cells were incubated with the primary antibody for 2 h and the signal was revealed with the Alexa Fluor® 594-conjugated antibody. For nuclear staining, cells were incubated with Hoechst 33342

at room temperature for 10 min. Images were obtained by using a confocal microscope (FV1000; Olympus). For quantification of LC3 dots, original images were deconvolved using ImageJ software. Data are expressed as the mean ± SD (LC3 dots per cell) of 3 different experiments. t test, *$P < 0.05$; **$P < 0.01$.

To identify autophagosomes, cells were co-transfected with a red fluorescent protein fused to LC3 (RFP-LC3) and shVMP1-EGFP expression vectors and fixed with 4% p-formaldehyde in PBS for 15 min. We consider an RFP-LC3 cell to have punctate staining when all the red fluorescence is present as punctate and no diffused protein remains. The cells were observed and photographed utilizing a confocal fluorescence microscope (FV1000; Olympus). The percentage of RFP-LC3 cells with punctate staining is the number of cells with punctate staining per 100 fluorescent RFP-LC3 transfected cells, which was determined in three independent experiments. For quantification, the number of fluorescent cells with punctate staining was counted in six random fields representing 100 fluorescent cells and expressed as the mean S.D. of the combined results. Experimental groups were compared using the t test for pairwise comparison ($n = 3$, ***$p < 0.001$).

Photodynamic therapy

CaCo2 and SW480 cells (12×10^4 cells per ml) were seeded in 96-well plates and kept in an incubator at 37 °C overnight. Cells were incubated with 1 mM Me-ALA for 4 h and then irradiated at 1, 2, 3, 4 and 5 J cm^{-2} ($n = 8$). Cells were irradiated employing a monochromatic light source (635 ± 17 nm) with a multi-LED system (coherent light) at an irradiation intensity of 1.65 mW cm^{-2} (as measured by using a Coherent Lasermate power meter). The culture medium was replaced with complete medium. After 24 h of treatment, 10 µl of MTT stock solution were added to each well containing 100 µl of complete medium. Cells were incubated with MTT for 4 h and formazan crystals were suspended in DMSO. The absorbance of the samples was read with a Multiskan FC photometer (Thermo Scientific) at 540 nm. The absorbance of control cells was considered as 100% of viability. When indicated, cells were subjected to PDT and treated with 100 nM WM, 5 mM 3-MA, 10 µM CQ, 100 nM rapamycin, and 200 µM CoCl$_2$, or transfected with shHIF-α or shVMP1 expression vectors. After 24 h, cell viability was measured by using the MTT assay. Cytotoxicity was expressed as the viability percentage of the control. When autophagic activators/inhibitors were employed in combination with PDT, optical density values from activator/inhibitor-treated cells without PDT were defined as 100% of viability. Analysis was carried out on normalized data by one-way ANOVA followed by Bonferroni's multiple comparison test. Data are expressed as the mean ± SD of 5 different experiments. *$P < 0.05$. When indicated, cell death was quantified with the trypan blue exclusion assay. Briefly, after 24 h of Me-ALA PDT, cells were trypsinized and incubated with 0.4% (w/v) trypan blue at room temperature for 10 min. Cells with trypan

blue uptake were counted as dead cells on a haemocytometer. Each individual experiment was repeated three times.

Statistical analysis

The results are expressed as mean ± SD. The present studies comply with the recommendations on experimental design and analysis in pharmacology.[31] We performed a minimum of five independent experiments, where individual data points were based on at least one technical duplicate. Different kinds of ANOVA models were applied to explore the differences between the groups of quantitative data. Repeated measures ANOVA was used to test for related, not independent groups of quantitative data. Two-way ANOVA was employed to compare the mean differences between groups that have been split into two independent variables. Two-way ANOVA with repeated measures on one of the factors was applied to test differences in experiments where the quantitative dependent variable was measured over two or more time points. Bonferroni was used as a *post hoc* test. *P* values less than 0.05 were considered statistically significant. Statistical analysis of data was performed using GraphPad Prism 6.

Results

HIF-1α induces autophagy in colon cancer cells

To explore whether HIF-1α is involved in autophagy induction in colon cancer cells we used the HIF-1α stabilizing agent cobalt chloride ($CoCl_2$). $CoCl_2$ promotes the stabilization of HIF-1α, which is normally hydroxylated and degraded by the proteasome system in the presence of molecular oxygen.[32] To standardize experimental conditions and ensure HIF-1α expression in our cell model, CaCo2 cells were treated with 100, 200 and 400 μM $CoCl_2$ for 24 h and HIF-1α levels were evaluated by western blotting. As shown in Fig. 1A, HIF-1α expression increases under 200 μM $CoCl_2$ treatment. We then evaluated the time required for the stabilization of HIF-1α. CaCo2 cells were treated with 200 μM $CoCl_2$ and HIF-1α levels were evaluated by immunoblotting after 6, 12 and 24 h post-treatment. As shown in Fig. 1B, HIF-1α expression increases after 24 h of $CoCl_2$ treatment. Next, the transcriptional activity of HIF-1 following $CoCl_2$ treatment was studied. After the dimerization of subunits α and β, HIF-1 recognizes HRE sequences, binds to promoter DNA and modulates the transcription of its target genes.[33] For this reason, we used the p5HRE-EGFP plasmid, which is a reporter vector of HIF-1 activity, that induces EGFP expression when HIF-1 is active.[34] CaCo2 cells were transiently transfected with p5HRE-EGFP and treated with 200 μM $CoCl_2$, and EGFP fluorescence was determined by confocal microscopy after 24 h. Fig. 1C shows that CaCo2 cells induce EGFP expression after $CoCl_2$ treatment. These results demonstrate that HIF-1 is stabilized and activated after 24 h $CoCl_2$ treatment in colon cancer cells.

To evaluate if HIF-1α promotes autophagy, we analyzed LC3 processing by immunoblotting following $CoCl_2$ treatment. During autophagy, the LC3 protein is processed from the

18 kDa to the 16 kDa form, which is recruited to the autophagosomal membrane. Therefore, increased LC3-II levels correlate with autophagy activation.[35] CaCo2 cells were incubated under control conditions and treated with 200 μM $CoCl_2$. Starving medium was used to induce autophagy and CQ treatment was used to inhibit the autophagy flux. Protein extracts were evaluated by immunoblotting after 24 h of incubation. Fig. 1D shows that after HIF-1α stabilization, autophagy was induced as is demonstrated by increased LC3-II levels. Moreover, the use of CQ in combination with $CoCl_2$ treatment induces LC3-II accumulation compared to $CoCl_2$- or CQ-alone treatment, supporting the fact that the autophagy flux is actually induced chemically by HIF-1 activation. Next, we performed the immunofluorescence of LC3 in cells incubated with $CoCl_2$. Starvation was used as a positive control of autophagy induction. Also, we used 3-MA, an inhibitor of the Class III PI3 K complex, in the initial steps of autophagy as a negative control. Fig. 1E shows the recruitment of LC3 in colon cancer cells under $CoCl_2$ treatment, which is abolished by 3-MA. To further confirm the role of HIF-1α in $CoCl_2$-induced autophagy, cells were transfected with a shRNAHIF-1α or shRNA-control vector before $CoCl_2$ treatment and the LC3 expression was analyzed by western blotting. As shown in Fig. 1F, LC3-II levels are reduced when HIF-1α is downregulated. Altogether, these data suggest a key role of HIF-1 in autophagy regulation in colon cancer cells.

Autophagy induced by HIF-1α is mediated by the expression of the autophagy-related protein VMP1

HIF-1α-induced autophagy has been reported in a wide variety of cancer cell lines,[36,37] including colon cancer cells.[38] However, the molecular mechanisms involved in HIF-1α-induced autophagy remain to be clarified.

VMP1 is an autophagosomal transmembrane protein that triggers autophagy even under nutrient-rich conditions.[23] To determine whether $CoCl_2$ treatment induces VMP1-mediated autophagy, we evaluate LC3 recruitment in CaCo2 cells transiently co-transfected with RFP-LC3 and shVMP1-EGFP and treated with $CoCl_2$. Fig. 2A shows that RFP-LC3 recruitment is not observed when VMP1 is downregulated in cells co-expressing shVMP1-EGFP and RFP-LC3, indicating that VMP1 is required for autophagy induction in response to HIF-1α stabilization. Fig. 2B shows the downregulation of VMP1 by shVMP1-EGFP.

We then explore whether HIF-1α is able to regulate the expression of VMP1. CaCo2 cells treated with 200 μM $CoCl_2$ for 24 h show increased VMP1 expression compared to untreated control cells. Moreover, cells treated with $CoCl_2$ after the silencing of HIF-1α with a specific shHIF-1α show significant reduction in VMP1 expression (Fig. 2C). The presence of three putative HIF-1α consensus-binding sites on the human VMP1 promoter sequence confirmed by *in silico* analysis suggests that HIF-1α is a potential transcription factor regulating VMP1 gene expression (Fig. 2D). Given that the activity of HIF-1α is necessary to induce VMP1 expression in $CoCl_2$-treated cells, we evaluated whether this effect is due to a direct
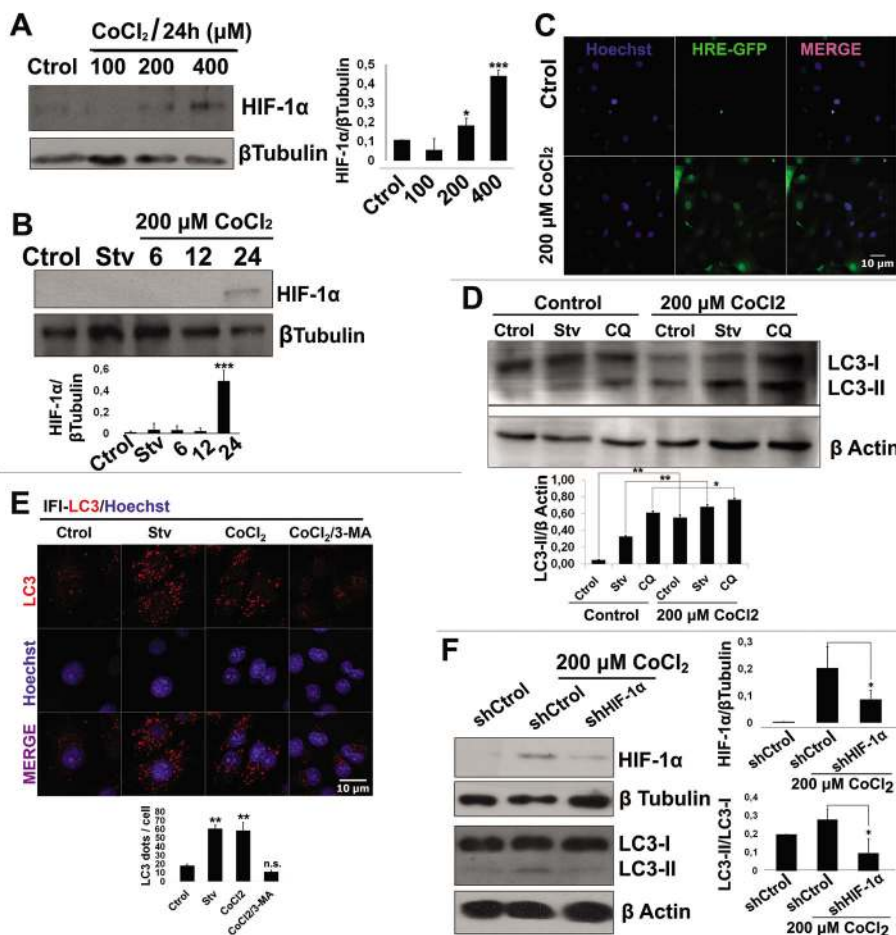
1634 | *Photochem. Photobiol. Sci.*, 2017, **16**, 1631–1642

This journal is © The Royal Society of Chemistry and Owner Societies 2017

Fig. 1 HIF-1α induces autophagy in colon cancer cells. (A) CaCo2 cells were treated with different doses of CoCl$_2$ (100, 200 or 400 μM) for 24 h and the expression of HIF-1α was detected by western blotting. Relative densitometry (HIF-1α/β-tubulin) is shown in the right panel ($n = 5$, *$p < 0.05$ vs. control, ***$p < 0.001$ vs. control). (B) Cells were treated with 200 μM CoCl$_2$ for 6, 12 or 24 h and the expression of HIF-1α was detected by western blotting. The lower panel shows relative densitometry (HIF-1α/β-tubulin) ($n = 5$, ***$p < 0.001$ vs. control). (C) CaCo2 cells were transiently transfected with the p5HRE-EGFP plasmid and treated with 200 μM CoCl$_2$ for 24 h. The transcriptional activity of HIF-1α was determined by analyzing the EGFP expression using a confocal microscope. Bar scale = 10 μm. (D) CaCo2 cells were incubated in control medium (Ctrol); starving medium (Stv) or chloroquine (CQ) with or without 200 μM CoCl$_2$ and LC3 expression was detected by western blotting. Starvation was used as a positive control of autophagy and CQ was used to inhibit the autophagic flux. The lower panel shows relative densitometry (LC3-II/β-actin) ($n = 5$, $p < 0.05$ **$p < 0.01$). (E) CaCo2 cells were starved (Stv) as an autophagy positive control, treated with 200 μM CoCl$_2$ or 200 μM CoCl$_2$ plus the autophagy inhibitor 3-methyladenine (3-MA). Autophagic vesicles were detected by indirect immunofluorescence (IFI) of LC3. Images were obtained using confocal microscopy. Representative images show the punctate LC3 in the cytoplasm indicating autophagy. Bar scale = 10 μm. Quantification of the number of LC3 dots per cell is shown in the lower panel ($n = 5$, n.s. = non-significant, **$p < 0.01$ vs. control). (F) Cells were transiently transfected with a control vector (shCtrol) or a shRNAHIF-1α vector (shHIF-1α), and treated with 200 μM CoCl$_2$ for 24 h. The expressions of HIF-1α and LC3 were analyzed by western blotting. Relative densitometries are shown in the right panel (HIF-1α/β-tubulin; LC3-II/LC3-I) ($n = 5$, *$p < 0.05$).

binding of HIF-1α to the VMP1 promoter. We performed a ChIP assay using chromatin immunoprecipitation from CaCo2 cells with a specific HIF-1α antibody and specific primers for putative binding sites of this factor in the VMP1 promoter sequence. Fig. 2E shows a positive amplification signal of HIF-1α to putative binding sites in the VMP1 promoter in anti-HIF-1α precipitates from CaCo2 cells subjected to 200 μM CoCl$_2$ treatment. These results demonstrate that HIF-1α binds directly to a region located 579 bp to 765 bp downstream of the beginning of the first intron of the VMP1 gene and confirm that HIF-1α is able to regulate VMP1 gene expression. Under CoCl$_2$ treatment, the percentage of input increases

3.4-fold compared to untreated cells. Altogether, these results demonstrate a new mechanism of autophagy induction in human tumor cells, in which VMP1 is a novel direct target of HIF-1α.

The HIF-1-induced autophagy confers resistance to PDT

Colon tumor cells are normally under hypoxic conditions and activate HIF-1α to survive in this hostile microenvironment. To investigate the effect of HIF-1α activation in the PDT context, we first performed a dose–response curve of Me-ALA/PDT in CaCo2 and SW480 cells. Me-ALA/PDT induces significant cytotoxicity in a light-dose dependent manner as indicated by the
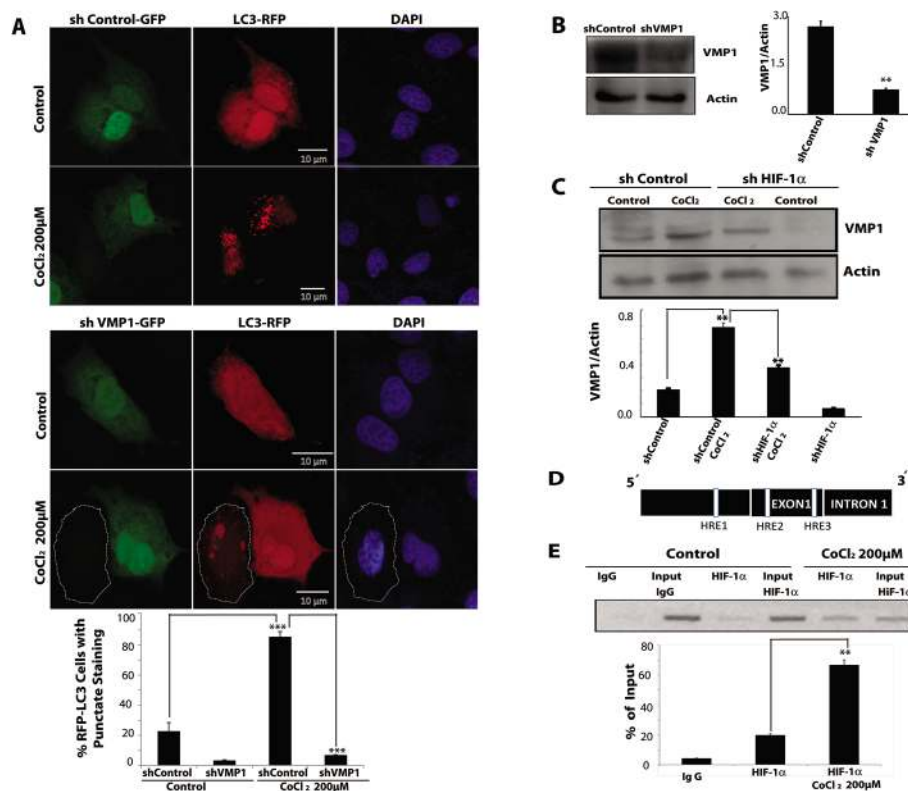
This journal is © The Royal Society of Chemistry and Owner Societies 2017

Photochem. Photobiol. Sci., 2017, **16**, 1631–1642 | **1635**

Fig. 2 Autophagy induced by HIF-1α is mediated by the expression of the autophagy-related protein VMP1. (A) CaCo2 cells were transiently co-transfected with RFP-LC3 and shVMP1-EGFP expression vectors, and they were treated with 200 μM CoCl₂ for 24 h. RFP-LC3 distribution was detected using confocal microscopy. Representative images show the punctate RFP-LC3 in cells EGFP− vs. EGFP+. The white circle shows the shVMP1-EGFP non-transfected cell. Bar scale = 10 μm. Quantitation represents the percentage of RFP-LC3 cells with punctate staining (n = 5, ***p < 0.001). (B) CaCo2 cells were transfected with the shControl or shVMP1 expression vector. VMP1 expression was detected by western blotting. Relative densitometry (VMP1/actin) is shown in the right panel (n = 5, **p < 0.01). (C) CaCo2 cells were transfected with shHIF-1α or shControl, and treated with 200 μM CoCl₂ for 24 h. Control cells were incubated in normal medium. VMP1 expression was detected by western blotting. Relative densitometry (VMP1/actin) is shown in the lower panel (n = 5, **p < 0.01). (D) Scheme showing 3 HRE consensus elements found in positions 59704668−59708628 on chromosome 17 of the human genome, which includes exon 1, intron 1 and the 2800 bp 5′ upstream sequence of exon 1 from the VMP1 gene. (E) Control CaCo2 cells and cells treated with 200 μM CoCl₂ for 24 h were lysed, and the chip assay was performed using a HIF-1α antibody. IgG is a negative control. PCR was performed using a specific set of primers as described under "Experimental". The positive amplicon for the chip assay was located 579 bp to 765 bp downstream of the beginning of the first intron (HRE3). Input is the total DNA of VMP1-promoter loading for each condition. Quantitation represents the percentage of the HIF-1α antibody bound to the VMP1 promoter relative to the input (% of input) (n = 5, **p < 0.01).

MTT assay (Fig. 3A). A sub-lethal dose (3 J cm^{-2} in CaCo2 cells and 2 J cm^{-2} in SW480 cells) was used for all the following experiments.

We then evaluated the role of HIF-1α in cell survival after PDT. Cells were incubated with 200 μM CoCl₂ and transiently transfected with shRNA HIF-1α to induce HIF-1α downregulation or shRNA control. As shown in Fig. 3B, HIF-1α stabilization significantly increases the cell survival rate in both cell lines after PDT. Interestingly, HIF-1α downregulation sensitizes CaCo2 and SW480 cells to the PDT effect. Moreover, we evaluated cell death by using the trypan blue exclusion assay 24 h after irradiation. As shown in Fig. 3C, the percentage of cell death is reduced in cells treated with CoCl₂, and HIF-1α downregulation significantly increases cell death in both cell lines. These results suggest that HIF-1α mediates resistance to PDT in these cells.

Then, we explored the role of HIF-1α-mediated autophagy induced by CoCl₂ treatment in colon cancer cells after PDT.

We treated CaCo2 and SW480 cells with rapamycin to induce autophagy, with CoCl₂, and with CoCl₂ plus 3-MA to inhibit autophagy. After 24 h of incubation, we evaluated cell viability and found that autophagy, induced either by rapamycin or by CoCl₂ treatment, promotes resistance to cell death under PDT (Fig. 3D). Remarkably, the inhibition of autophagy in cells treated with CoCl₂ sensitizes both cell lines to the photodynamic effect. Altogether, our findings suggest that HIF-1α-induced autophagy is able to promote cancer cell resistance to PDT.

Autophagy induced by PDT promotes resistance in colon cancer cells

Above, we demonstrated that autophagy induced by HIF-1α confers resistance to PDT. Next, we evaluated the effect of PDT on autophagy. CaCo2 and SW480 cells were treated with Me-ALA/PDT and the autophagic flux was evaluated by immuno-
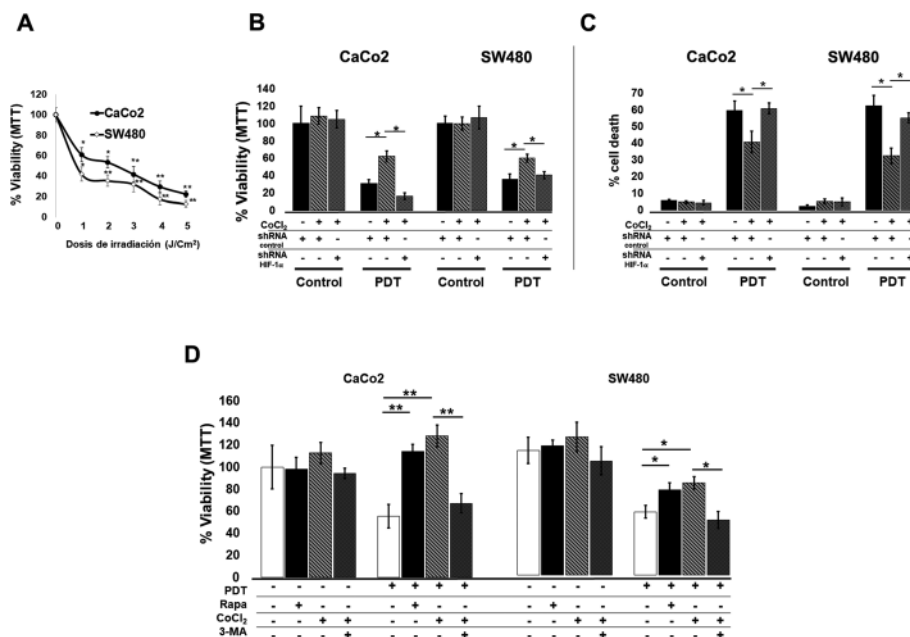
1636 | Photochem. Photobiol. Sci., 2017, **16**, 1631–1642

This journal is © The Royal Society of Chemistry and Owner Societies 2017

Fig. 3 HIF-1-induced autophagy confers resistance to PDT. (A) CaCo2 and SW480 cells were incubated with 1 mM ME-ALA for 4 h followed by irradiation with different light doses (1, 2, 3, 4 or 5 J cm^{-2}). Cell viability was evaluated by using the MTT assay 24 h after irradiation. The control group (0 J cm^{-2}) was considered 100% of viability for each cell line. Data were obtained from five independent experiments and are shown as mean ± SD (*$p < 0.05$, **$p < 0.01$). (B) Cell survival rate of CaCo2 and SW480 cells transiently transfected with a control vector (shCtrol) or shRNAHIF-1α vector (shHIF-1α) and pre-treated with 200 μm CoCl$_2$. All groups were treated or not with ME-ALA/PDT (irradiation doses: CaCo2: 3 J cm^{-2}; SW480: 2 J cm^{-2}). Cell viability was assessed by MTT 24 h after irradiation. The percentage of viability was calculated for each group treated with PDT, relative to their control (non-treated with PDT). Data were obtained from five independent experiments and are shown as mean ± SD (*$p < 0.05$). (C) CaCo2 and SW480 cells were transiently transfected with a control vector (shCtrol) or shRNAHIF-1α vector (shHIF-1α) and pre-treated with 200 μm CoCl$_2$. The groups were treated or not with ME-ALA/PDT (irradiation doses: CaCo2: 3 J cm^{-2}; SW480: 2 J cm^{-2}). Cell death was determined using the trypan blue exclusion assay 24 h after irradiation. Quantitation represents the percentage of trypan blue positive cells (dead cells). Data are shown as mean ± SD of five independent experiments (*$p < 0.05$, **$p < 0.01$). (D) Cell survival rate of CaCo2 and SW480 cells pre-treated with 100 nM rapamycin (RAPA), 200 μM CoCl$_2$ or 200 μM CoCl$_2$ plus 10 mM 3-methyladenine (3-MA) and treated or not with ME-ALA/PDT. The percentage of viability was calculated for each group treated with PDT, relative to their control (non-treated with PDT). Data were obtained from five independent experiments and are shown as mean ± SD (*$p < 0.05$; **$p < 0.01$).

blotting and fluorescence microscopy analysis in a time course after treatment. As shown in Fig. 4A and B, LC3-II levels increase 3 h and 30 min after PDT in CaCo2 and SW480 cells, respectively. In order to evaluate the autophagic flux, we determined the integrity of p62/SQSTM1, which is selectively degraded by autophagy.[39] Accordingly, decreased levels of p62/SQSTM1 expression are observed in both cell lines in a time dependent manner, indicating an increased autophagic flux after treatment. Moreover, LC3 aggregates in puncta 30 min after PDT compared to control cells without treatment (Fig. 4C). Therefore, PDT induces autophagy in colon cancer cells.

We then studied the role of autophagy in the PDT context. CaCo2 and SW480 cells were incubated with Me-ALA and several inhibitors of autophagy for 4 h, and an LD50 irradiation dose was applied. Fig. 5A shows the experimental design. As shown in Fig. 5B, 3-MA blocks the LC3-II conversion and CQ pre-treatment induces an exacerbated accumulation of the LC3-II form confirming that the autophagic flux is induced under PDT in colon cancer cells. Next, we evaluated the cell viability by using the MTT and trypan blue exclusion assays. Fig. 5C shows that autophagy inhibition with 3-MA, wortman-

nin (WM) or CQ photosensitizes both cell lines to photodamage effects. Furthermore, as shown in Fig. 5D, the percentage of cell death was higher when autophagy was inhibited in both cell lines. Altogether, our results indicate that PDT-induced autophagy mediates resistance to PDT in colon cancer cells.

HIF-1α/VMP1-autophagic pathway mediates PDT resistance in colon cancer cells

So far, we demonstrated that the HIF-1α/VMP1-autophagic pathway is induced by CoCl$_2$ in colon cancer cells and confers resistance to PDT. Next, we evaluated the effect of PDT on this new pathway. HIF-1α was assayed by immunoblotting at multiple time points after PDT. As shown in Fig. 6A, HIF-1α expression was induced after 1 h post-PDT. Then, CaCo2 cells were transiently transfected with a shHIF-1α or control vector and LC3 conversion was evaluated by immunoblotting following PDT. Interestingly, the downregulation of HIF-1α decreases LC3-II conversion after PDT (Fig. 6B). This suggests that PDT induces HIF-1α stabilization which, in turn, promotes autophagy. Then, we analyzed the role of VMP1 in the PDT context. As shown in Fig. 6C, VMP1 protein expression is induced after

This journal is © The Royal Society of Chemistry and Owner Societies 2017

Photochem. Photobiol. Sci., 2017, **16**, 1631–1642 | **1637**
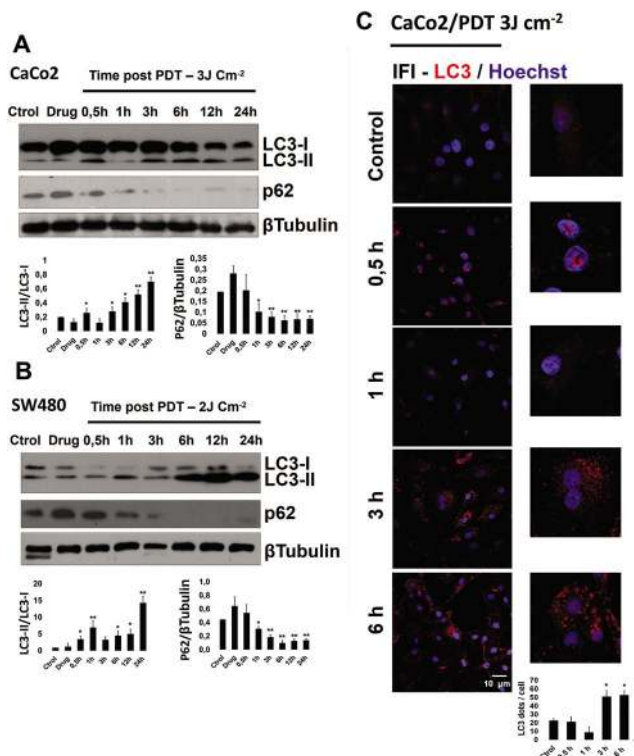
Fig. 4 Photodynamic therapy induces autophagy in colon cancer cells. (A, B) CaCo2 and SW480 cells were treated with 1 mM ME-ALA/PDT and protein extraction was realized at different time points after therapy. LC3 and p62/SQSTM1 expressions were analyzed by western blotting (Ctrol: untreated cells; Drug: ME-ALA without irradiation). The lower panel shows relative densitometry (LC3-II/LC3-I and p62/β-tubulin) ($n = 5$, *$p < 0.05$ vs. control; **$p < 0.01$ vs. control). (C) CaCo2 cells were incubated with 1 mM ME-ALA for 4 h and then irradiated with 3 J cm^{-2}. Autophagic vesicles (av) were detected by indirect immunofluorescence (IFI) of LC3. Images were obtained by using a confocal microscope. Representative images showed the punctate LC3 at different time points after treatment. The lower panel shows the quantification of the number of LC3 dots per cell ($n = 5$, *$p < 0.05$ vs. control; **$p < 0.01$ vs. control).
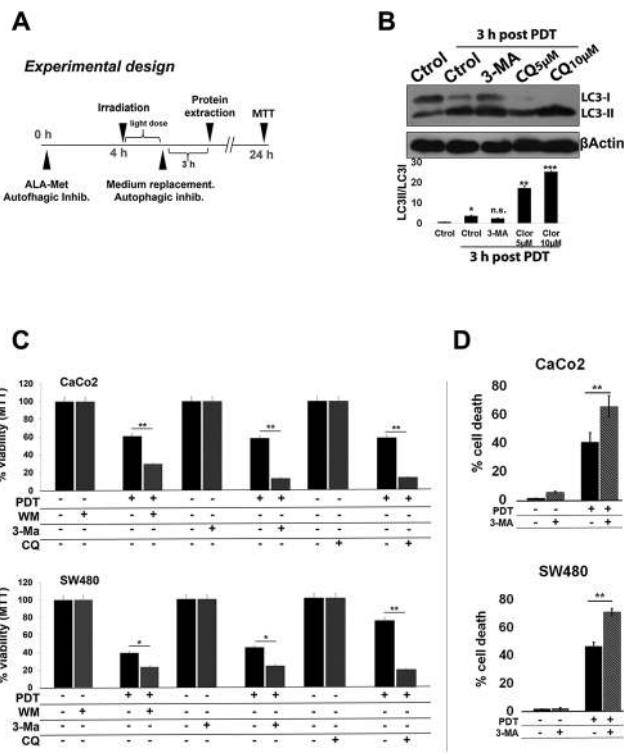
Fig. 5 Autophagy induced by PDT promotes resistance in colon cancer cells. (A) Schema of the experimental design. (B) CaCo2 cells were pre-treated with 5 mM 3-methyladenine (3-MA) or chloroquine (CQ) (5 μM or 10 μM) before ME-ALA/PDT treatment. Protein extraction was realized at 3 h after PDT and LC3 level was evaluated by western blotting. The lower panel shows relative densitometry (LC3-II/LC3-I) ($n = 5$, n.s. = non-significant, *$p < 0.05$ vs. control; **$p < 0.01$ vs. control, ***$p < 0.001$ vs. control). (C) CaCo2 and SW480 cells incubated with 10 μM wortmannin (WM), 5 mM 3-MA or 10 μM CQ were treated with PDT. After irradiation, the medium was replaced with a medium with autophagic inhibitors for 4 h. Cell viability was evaluated by using the MTT assay 24 h after irradiation. Values are expressed as a percentage of viability relative to the control group without PDT. Data were obtained from five independent experiments and are shown as mean ± SD (*$p < 0.05$; **$p < 0.01$). (D) CaCo2 and SW480 cells were incubated with 5 mM 3-MA and treated with PDT (irradiation doses: CaCo2: 3 J cm^{-2}; SW480: 2 J cm^{-2}). After irradiation, the medium was replaced with a medium with autophagic inhibitors for 4 h. Cell death was assessed by using the trypan blue exclusion assay 24 h after irradiation. Quantitation represents the percentage of trypan blue positive cells (dead cells). Data are expressed as mean ± SD of five independent experiments (*$p < 0.05$, **$p < 0.01$).

PDT. Also, we explored if VMP1 modulates PDT-induced autophagy. CaCo2 cells transiently co-transfected with RFP-LC3 and shVMP1-EGFP were treated with PDT, and LC3 recruitment was analyzed by using a fluorescence microscope. As shown in Fig. 6D, RFP-LC3 remains diffuse in cells expressing shVMP1-EGFP compared to RFP-LC3 alone after PDT, indicating that VMP1-mediated autophagy is induced by PDT. Accordingly, as shown in Fig. 6E, the downregulation of VMP1 also decreased LC3 processing after PDT, which is similar to the early-stage inhibition of autophagy by 3-MA. These results indicate that PDT induces autophagy in a VMP1 dependent manner.

Finally, we evaluated the role of VMP1 in cell survival after PDT. Cells were transiently transfected with the shVMP1-EGFP or shControl vector and cell viability was determined after PDT by using the MTT assay. As shown in Fig. 6F, the downregulation of VMP1 sensitizes cells to PDT. Altogether, these findings strongly suggest that the HIF-1α/VMP1-autophagic pathway is induced by PDT and acts as a survival mechanism in colon cancer cells.

Discussion

Hypoxia is a widely studied factor promoting cancer cell chemo/radioresistance[40] and, in the last decade, it has been implicated in the resistance to PDT protocols.[41,42] Autophagy has also been proposed as a common mechanism of resistance to chemotherapy and targeted therapies including PDT.[21,43]

It was suggested that autophagy is a common response to PDT and it is involved in either cell survival or cell death.[21] On the other hand, it was shown that PDT is able to induce the stabilization and activation of HIF-1α.[44] Nevertheless, the implication of HIF-1 as a modulator of autophagy in response

1638 | Photochem. Photobiol. Sci., 2017, 16, 1631–1642

This journal is © The Royal Society of Chemistry and Owner Societies 2017
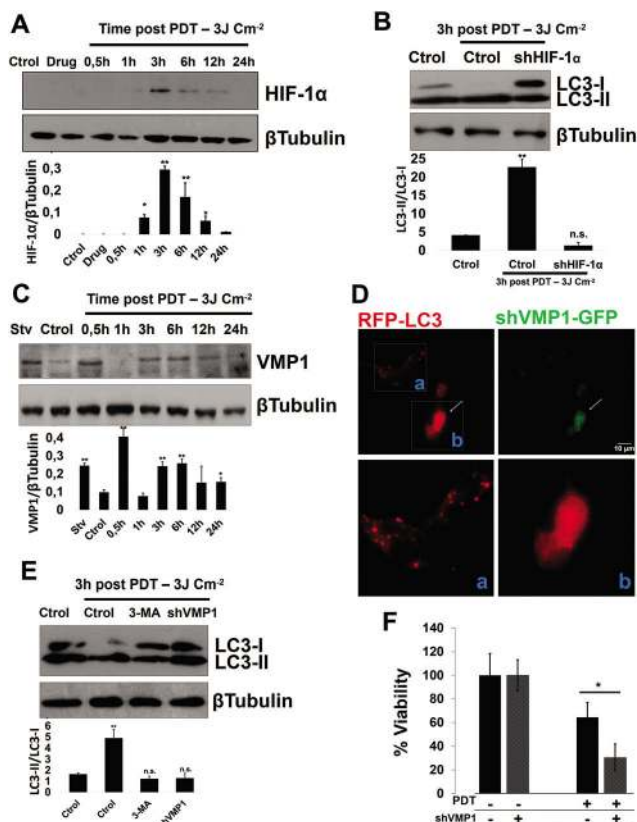
Fig. 6 HIF-1α/VMP1-autophagic pathway mediates PDT resistance in colon cancer cells. (A) CaCo2 cells were treated with ME-ALA/PDT and protein extraction was realized at different time points after therapy. HIF-1α expression was analyzed by western blotting (Ctrol: untreated cells; Drug: ME-ALA without irradiation). The lower panel shows relative densitometry (HIF-1α/β-tubulin) ($n = 5$, *$p < 0.05$ vs. control; **$p < 0.01$ vs. control). (B) CaCo2 cells were transiently transfected with a control vector (Ctrol) or shRNAHIF-1α vector (shHIF-1α) and treated with ME-ALA/PDT. 3 h post-therapy, LC3 expression was detected by western blotting. The lower panel shows relative densitometry (LC3-II/LC3-I). ($n = 5$, n.s. = non-significant, **$p < 0.01$ vs. control). (C) CaCo2 cells were treated with ME-ALA/PDT and protein extraction was realized at different time points after therapy. VMP1 protein expression was evaluated by western blotting (Ctrol: untreated cells; Stv: starved cells). The lower panel shows relative densitometry (VMP1/β-tubulin) ($n = 5$, *$p < 0.05$ vs. control, **$p < 0.01$ vs. control). (D) CaCo2 cells co-transfected with shVMP1-EGFP and RFP-LC3 expression vectors were treated with ME-ALA/PDT. RFP-LC3 distribution was evaluated and photographed by using a fluorescence microscope 3 h post-therapy. Representative images show the punctate RFP-LC3 in cells EGFP− (inset a) vs. EGFP+ (inset b). The white arrow shows shVMP1-GFP-expresing cells. Bar scale = 10 μm. (E) Cells were transiently transfected with a control vector (Ctrol) or shVMP1-EGFP vector (shVMP1) and treated with ME-ALA/PDT. LC3 expression was detected 3 h post-therapy by western blotting. The lower panel shows relative densitometry (LC3-II/LC3-I) ($n = 5$, **$p < 0.01$ vs. control). (F) Cell survival rate of CaCo2 cells transiently transfected with a control or shVMP1-EGFP vector before ME-ALA/PDT. Cell viability was assessed by MTT 24 h after irradiation. The percentage of viability was calculated for each group treated with PDT, relative to their control (non-treated with PDT). Data were obtained from five independent experiments and are shown as mean ± SD (*$p < 0.05$).

to PDT has not been elucidated. Previously, we proposed the possible effects of PDT on tumor microenvironment, in which it is stated that HIF-1 might trigger autophagy as a survival mechanism.[45] Here, we show that colon cancer cells efficiently induce the protein expression and transcriptional activity of HIF-1 under CoCl$_2$ treatment. Also, notable induction of autophagy is dependent on HIF-1α after CoCl$_2$ treatment suggesting that HIF-1 is an efficient player to modulate autophagy in colon cancer cells. Our results are consistent with reports suggesting that HIF-1 is able to induce autophagy[37,46] and other studies suggesting that, under hypoxic-mimic conditions, cancer cells are more resistant to PDT in a HIF-1 dependent manner.[42]

Our data reveal that HIF-1α is critical for CoCl$_2$-induced PDT resistance, since cancer cells incubated with CoCl$_2$ showed a higher percentage of cell survival compared to control cells under PDT. Moreover, we demonstrated that CoCl$_2$ promotes resistance to PDT through autophagy induction, because the inhibition of autophagy under conditions where HIF-1α is stabilized increases cell sensitization to PDT. We show that PDT induces a significant increase of autophagic flux in both CaCo2 and SW480 cells. Interestingly, when colon cancer cells were treated with autophagy inhibitors such as 3-MA, WM or CQ, the currently available autophagy pharmacological inhibitors,[47] they became sensitive to PDT. The inhibitor 3-MA can affect cell survival in an autophagy independent manner through AKT and other kinases.[48] It has also been reported that CQ can inhibit cell growth and promote cell death in cancer cells.[49,50] However, under our model conditions, we did not observe cytotoxic effects when colon cancer cells were treated with 3-MA, WM or CQ alone.

The autophagy-related protein VMP1 is required for autophagosome formation in mammalian cells under all conditions and its expression triggers autophagy even under nutrient-rich conditions.[23,27] VMP1 binds directly to the BH3 domain of Beclin-1 promoting the dissociation of Bcl-2 from Beclin-1 and the activation of the Class III PI3 K complex to initiate the autophagosome formation.[25,26] Previously, we demonstrated that VMP1 is induced by gemcitabine in pancreatic cancer cells[29] and that the AKT1-GLI3-VMP1 pathway mediates KRAS oncogene-induced autophagy in pancreatic cancer cells.[28] Other authors suggested that VMP1 expression can also be modulated by a HIF-1/miR-210 pathway in ovarian cancer cells.[51] Here we demonstrate that VMP1 is induced under HIF-1α stabilization. We found three HRE consensus sequences in positions 59704668–59708628 on chromosome 17 of the human genome, which includes exon 1, intron 1 and 2800 bp 5′ upstream sequence of exon 1, and ChIP assays show direct binding of HIF-1α to the VMP1 promoter. Our results indicate that VMP1 is a novel direct target of HIF-1α and its expression mediates HIF-1α-induced autophagy. Therefore, we propose a key role of HIF-1α in the initiation steps of VMP1-related autophagy in colon cancer cells.

It is possible that autophagy attempts to remove organelles damaged by oxidation or to degrade large aggregates of cross-linked proteins. Thus, ROS produced by the photodynamic

This journal is © The Royal Society of Chemistry and Owner Societies 2017

Photochem. Photobiol. Sci., 2017, **16**, 1631–1642 | **1639**

treatment could be involved in autophagy induction.[52] PDT may result in a temporal photochemical consumption of molecular oxygen.[53,54] Moreover, PDT-induced ROS may evoke HIF-1α stabilization and activation.[55–57] In this sense, our results have demonstrated that PDT significantly increased the expression of HIF-1α in colon cancer cells. In addition, when HIF-1α is downregulated, cells become sensitive to PDT, indicating that PDT induces HIF-1α as a survival mechanism during treatment.

Altogether, our results indicate that PDT, employing Me-ALA as the photosensitizer, induces autophagy as a resistance mechanism. It has been shown that tumor resistance to PDT can be induced through the upregulation of autophagy using other photosensitizers.[58,59] In this sense, while our results showed that HIF-1-autophagy can work together under our experimental conditions (CoCl$_2$/PDT context), we cannot rule out the possibility that autophagy might be induced by HIF-1 independent mechanisms in response to PDT.[60] Further investigation on other mechanisms of resistance mediated by autophagy (*e.g.* by rapamycin or cDNA-VMP1) under conditions where HIF-1 is downregulated would be of interest.

Finally, we demonstrated that HIF-1α and VMP1 are involved in PDT-induced autophagy. Our study showed that both HIF-1α and VMP1 are markedly increased following PDT. It is interesting to note that the VMP1 kinetic expression seems to be biphasic. This might be explained considering that VMP1 is a stress protein which is rapidly expressed by pre-formed RNA. Moreover, the downregulation of HIF-1α or VMP1 decreases LC3 processing and inhibits LC3 puncta formation after PDT, which confirm that the HIF-1/VMP1 axis is required for PDT-induced autophagy. To our knowledge, this is the first report showing that PDT-induced autophagy is directly mediated by HIF-1α and linked to VMP1 as a PDT-induced resistance mechanism.

Conclusions

The present study has demonstrated that PDT resistance in colon cancer cells under CoCl$_2$ treatment is mediated by the induction of a novel HIF-1α/VMP1-autophagic pathway, which could be exacerbated by PDT effects (Fig. 7). Further studies focusing on the potential clinical application of this molecular mechanism of tumor cell resistance will provide novel strategies of PDT protocols for colon cancer.

Conflicts of interest

There are no conflicts of interest to declare.

Acknowledgements

Fig. 7 Schematic model. HIF-1α/VMP1-induced autophagy confers resistance to cell death under PDT.

References

1 D. L. Longo and W. B. Strum, Colorectal Adenomas, *N. Engl. J. Med.*, 2016, **374**(11), 1065–1075.

2 K. De Greef, C. Rolfo, A. Russo, *et al.*, Multisciplinary management of patients with liver metastasis from colorectal cancer, *World J. Gastroenterol.*, 2016, **22**(32), 7215–7225.

3 R. M. Heaney, C. Shields and J. Mulsow, Outcome following incomplete surgical cytoreduction combined with intraperitoneal chemotherapy for colorectal peritoneal metastases, *World J. Gastrointest. Oncol.*, 2015, **7**(12), 445–454.

4 S. B. Brown, E. A. Brown and I. Walker, The present and future role of photodynamic therapy in cancer treatment, *Lancet Oncol.*, 2004, **5**(8), 497–508.

5 A. Oniszczuk, K. A. Wojtunik-Kulesza, T. Oniszczuk and K. Kasprzak, The potential of photodynamic therapy (PDT) —Experimental investigations and clinical use, *Biomed. Pharmacother.*, 2016, **83**, 912–929.

6 A. P. Castano, T. N. Demidova and M. R. Hamblin, Mechanisms in photodynamic therapy: part two—cellular signaling, cell metabolism and modes of cell death, *Photodiagn. Photodyn. Ther.*, 2005, **2**(1), 1–23.
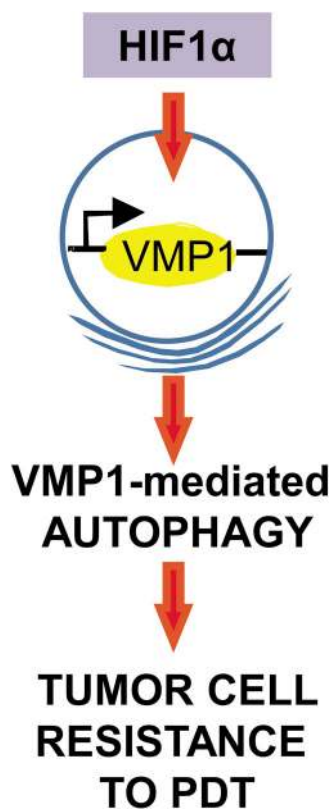
7 J.-O. Yoo and K.-S. Ha, New insights into the mechanisms for photodynamic therapy-induced cancer cell death, *Int. Rev. Cell Mol. Biol.*, 2012, **295**, 139–174.

8 N. Shishkova, O. Kuznetsova and T. Berezov, Photodynamic therapy in gastroenterology, *J. Gastrointest. Cancer*, 2013, **44**(3), 251–259.

9 H. Barr, A. J. MacRobert, C. J. Tralau, P. B. Boulos and S. G. Bown, The significance of the nature of the photosensitizer for photodynamic therapy: quantitative and biological studies in the colon, *Br. J. Cancer*, 1990, **62**(5), 730–735.

10 J.-P. Cosse and C. Michiels, Tumour hypoxia affects the responsiveness of cancer cells to chemotherapy and promotes cancer progression, *Anticancer Agents Med. Chem.*, 2008, **8**(7), 790–797.

11 K. Balamurugan, HIF-1 at the crossroads of hypoxia, inflammation, and cancer, *Int. J. Cancer*, 2016, **138**(5), 1058–1066.

12 C. Michiels, C. Tellier and O. Feron, Cycling hypoxia: A key feature of the tumor microenvironment, *Biochim. Biophys. Acta, Rev. Cancer*, 2016, **1866**(1), 76–86.

13 I. Amelio and G. Melino, The p53 family and the hypoxia-inducible factors (HIFs): determinants of cancer progression, *Trends Biochem. Sci.*, 2015, **40**(8), 425–434.

14 L. Lin and E. H. Baehrecke, Autophagy, cell death, and cancer, *Mol. Cell. Oncol.*, 2015, **2**(3), e985913.

15 L. Harhaji-Trajkovic, U. Vilimanovich, T. Kravic-Stevovic, V. Bumbasirevic and V. Trajkovic, AMPK-mediated autophagy inhibits apoptosis in cisplatin-treated tumour cells, *J. Cell. Mol. Med.*, 2009, **13**(9B), 3644–3654.

16 D. Liu, Y. Yang, Q. Liu and J. Wang, Inhibition of autophagy by 3-MA potentiates cisplatin-induced apoptosis in esophageal squamous cell carcinoma cells, *Med. Oncol.*, 2011, **28**(1), 105–111.

17 B. Del Bello, M. Toscano, D. Moretti and E. Maellaro, Cisplatin-induced apoptosis inhibits autophagy, which acts as a pro-survival mechanism in human melanoma cells, *PLoS One*, 2013, **8**(2), e57236.

18 A. Terman and U. T. Brunk, Autophagy in cardiac myocyte homeostasis, aging, and pathology, *Cardiovasc. Res.*, 2005, **68**(3), 355–365.

19 X. Yang, D.-D. Yu, F. Yan, *et al.*, The role of autophagy induced by tumor microenvironment in different cells and stages of cancer, *Cell Biosci.*, 2015, **5**(1), 14.

20 A. François, S. Marchal, F. Guillemin and L. Bezdetnaya, mTHPC-based photodynamic therapy induction of autophagy and apoptosis in cultured cells in relation to mitochondria and endoplasmic reticulum stress, *Int. J. Oncol.*, 2011, **39**(6), 1537–1543.

21 T. R. O'Donovan, G. C. O'Sullivan and S. L. McKenna, Induction of autophagy by drug-resistant esophageal cancer cells promotes their survival and recovery following treatment with chemotherapeutics, *Autophagy*, 2011, **7**(5), 509–524.

22 M.-F. Wei, M.-W. Chen, K.-C. Chen, *et al.*, Autophagy promotes resistance to photodynamic therapy-induced apoptosis selectively in colorectal cancer stem-like cells, *Autophagy*, 2014, **10**(7), 1179–1192.

23 A. Ropolo, D. Grasso, R. Pardo, *et al.*, The pancreatitis-induced vacuole membrane protein 1 triggers autophagy in mammalian cells, *J. Biol. Chem.*, 2007, **282**(51), 37124–37133.

24 M. I. Vaccaro, A. Ropolo, D. Grasso and J. L. Iovanna, A novel mammalian trans-membrane protein reveals an alternative initiation pathway for autophagy, *Autophagy*, 2008, **4**(3), 388–390.

25 M. I. Molejon, A. Ropolo and M. I. Vaccaro, VMP1 is a new player in the regulation of the autophagy-specific phosphatidylinositol 3-kinase complex activation, *Autophagy*, 2013, **9**(6), 933–935.

26 M. I. Molejon, A. Ropolo, A. Lo Re, V. Boggio and M. I. Vaccaro, The VMP1-Beclin 1 interaction regulates autophagy induction, *Sci. Rep.*, 2013, **3**, 1055.

27 D. Grasso, A. Ropolo, A. Lo Ré, *et al.*, Zymophagy, a novel selective autophagy pathway mediated by VMP1-USP9x-p62, prevents pancreatic cell death, *J. Biol. Chem.*, 2011, **286**(10), 8308–8324.

28 A. E. Lo Ré, M. G. Fernández-Barrena, L. L. Almada, *et al.*, Novel AKT1-GLI3-VMP1 pathway mediates KRAS oncogene-induced autophagy in cancer cells, *J. Biol. Chem.*, 2012, **287**(30), 25325–25334.

29 R. Pardo, A. Lo Ré, C. Archange, *et al.*, Gemcitabine induces the VMP1-mediated autophagy pathway to promote apoptotic death in human pancreatic cancer cells, *Pancreatology*, 2010, **10**(1), 19–26.

30 D. Vordermark, P. Kraft, A. Katzer, *et al.*, Glucose requirement for hypoxic accumulation of hypoxia-inducible factor-1alpha (HIF-1alpha), *Cancer Lett.*, 2005, **230**(1), 122–133.

31 M. J. Curtis, R. A. Bond, D. Spina, *et al.*, Experimental design and analysis and their reporting: new guidance for publication in BJP, *Br. J. Pharmacol.*, 2015, **172**(14), 3461–3471.

32 L. M. Lopez-Sánchez, C. Jimenez, A. Valverde, *et al.*, CoCl$_2$, a mimic of hypoxia, induces formation of polyploid giant cells with stem characteristics in colon cancer, *PLoS One*, 2014, **9**(6), e99143, Maki CG, ed.

33 E. L. LaGory and A. J. Giaccia, The ever-expanding role of HIF in tumour and stromal biology, *Nat. Cell Biol.*, 2016, **18**(4), 356–365.

34 T. Shibata, A. J. Giaccia and J. M. Brown, Development of a hypoxia-responsive vector for tumor-specific gene therapy, *Gene Ther.*, 2000, **7**(6), 493–498.

35 Y. Kabeya, N. Mizushima, T. Ueno, *et al.*, LC3, a mammalian homologue of yeast Apg8p, is localized in autophagosome membranes after processing, *EMBO J.*, 2000, **19**(21), 5720–5728.

36 S. Wilkinson, J. O'Prey, M. Fricker and K. M. Ryan, Hypoxia-selective macroautophagy and cell survival signaled by autocrine PDGFR activity, *Genes Dev.*, 2009, **23**(11), 1283–1288.

37 Y. Sun, X. Xing, Q. Liu, *et al.*, Hypoxia-induced autophagy reduces radiosensitivity by the HIF-1α/miR-210/Bcl-2 pathway in colon cancer cells, *Int. J. Oncol.*, 2015, **46**(2), 750–756.

This journal is © The Royal Society of Chemistry and Owner Societies 2017

Photochem. Photobiol. Sci., 2017, **16**, 1631–1642 | **1641**

38 M. B. Gariboldi, E. Taiana, M. C. Bonzi, et al., The BH3-mimetic obatoclax reduces HIF-1α levels and HIF-1 transcriptional activity and sensitizes hypoxic colon adenocarcinoma cells to 5-fluorouracil, Cancer Lett., 2015, 364(2), 156–164.

39 D. J. Klionsky, The molecular machinery of autophagy: unanswered questions, J. Cell. Sci., 2005, 118(Pt 1), 7–18.

40 J. M. Brown and W. R. Wilson, Exploiting tumour hypoxia in cancer treatment, Nat. Rev. Cancer, 2004, 4(6), 437–447.

41 Z. Ji, G. Yang, S. Shahzidi, et al., Induction of hypoxia-inducible factor-1alpha overexpression by cobalt chloride enhances cellular resistance to photodynamic therapy, Cancer Lett., 2006, 244(2), 182–189.

42 A. Casas, G. Di Venosa, T. Hasan and Al Batlle, Mechanisms of resistance to photodynamic therapy, Curr. Med. Chem., 2011, 18(16), 2486–2515.

43 X.-H. Ma, S. Piao, D. Wang, et al., Measurements of tumor cell autophagy predict invasiveness, resistance to chemotherapy, and survival in melanoma, Clin. Cancer Res., 2011, 17(10), 3478–3489.

44 S. Mitra, S. E. Cassar, D. J. Niles, J. A. Puskas, J. G. Frelinger and T. H. Foster, Photodynamic therapy mediates the oxygen-independent activation of hypoxia-inducible factor 1alpha, Mol. Cancer Ther., 2006, 5(12), 3268–3274.

45 L. Milla Sanabria, M. E. Rodríguez, I. S. Cogno, et al., Direct and indirect photodynamic therapy effects on the cellular and molecular components of the tumor microenvironment, Biochim. Biophys. Acta, 2013, 1835(1), 36–45.

46 A. Tittarelli, B. Janji, K. Van Moer, M. Z. Noman and S. Chouaib, The selective degradation of synaptic connexin 43 protein by hypoxia-induced autophagy impairs natural killer cell-mediated tumor cell killing, J. Biol. Chem., 2015, 290(39), 23670–23679.

47 D. J. Klionsky, K. Abdelmohsen, A. Abe, et al., Guidelines for the use and interpretation of assays for monitoring autophagy (3rd edition), Autophagy, 2016, 12(1), 1–222.

48 B. Levine and J. Yuan, Autophagy in cell death: an innocent convict?, J. Clin. Invest., 2005, 115(10), 2679–2688.

49 P. Maycotte, S. Aryal, C. T. Cummings, J. Thorburn, M. J. Morgan and A. Thorburn, Chloroquine sensitizes breast cancer cells to chemotherapy independent of autophagy, Autophagy, 2012, 8(2), 200–212.

50 C. Fan, W. Wang, B. Zhao, S. Zhang and J. Miao, Chloroquine inhibits cell growth and induces cell death in

51 T. Liu, L. Zhao, W. Chen, et al., Inactivation of von Hippel-Lindau increases ovarian cancer cell aggressiveness through the HIF1α/miR-210/VMP1 signaling pathway, Int. J. Mol. Med., 2014, 33(5), 1236–1242.

52 R. Scherz-Shouval, E. Shvets, E. Fass, H. Shorer, L. Gil and Z. Elazar, Reactive oxygen species are essential for autophagy and specifically regulate the activity of Atg4, EMBO J., 2007, 26(7), 1749–1760.

53 T. H. Foster, R. S. Murant, R. G. Bryant, R. S. Knox, S. L. Gibson and R. Hilf, Oxygen consumption and diffusion effects in photodynamic therapy, Radiat. Res., 1991, 126(3), 296–303.

54 T. M. Sitnik, J. A. Hampton and B. W. Henderson, Reduction of tumour oxygenation during and after photodynamic therapy in vivo: effects of fluence rate, Br. J. Cancer, 1998, 77(9), 1386–1394.

55 S.-N. Jung, W. K. Yang, J. Kim, et al., Reactive oxygen species stabilize hypoxia-inducible factor-1 alpha protein and stimulate transcriptional activity via AMP-activated protein kinase in DU145 human prostate cancer cells, Carcinogenesis, 2008, 29(4), 713–721.

56 J. Y. Lee, S. A. Hirota, L. E. Glover, G. D. Armstrong, P. L. Beck and J. A. MacDonald, Effects of nitric oxide and reactive oxygen species on HIF-1a stabilization following Clostridium difficile toxin exposure of the Caco-2 epithelial cell line, Cell. Physiol. Biochem., 2013, 32(2), 417–430.

57 Y.-N. Li, M.-M. Xi, Y. Guo, C.-X. Hai, W.-L. Yang and X.-J. Qin, NADPH oxidase-mitochondria axis-derived ROS mediate arsenite-induced HIF-1α stabilization by inhibiting prolyl hydroxylases activity, Toxicol. Lett., 2014, 224(2), 165–174.

58 M. Dewaele, W. Martinet, N. Rubio, et al., Autophagy pathways activated in response to PDT contribute to cell resistance against ROS damage, J. Cell. Mol. Med., 2011, 15(6), 1402–1414.

59 P. Tu, Q. Huang, Y. Ou, et al., Aloe-emodin-mediated photodynamic therapy induces autophagy and apoptosis in human osteosarcoma cell line MG-63 through the ROS/JNK signaling pathway, Oncol. Rep., 2016, 35(6), 3209–3215.

60 H. Choi, C. Merceron, L. Mangiavini, et al., Hypoxia promotes noncanonical autophagy in nucleus pulposus cells independent of MTOR and HIF1A signaling, Autophagy, 2016, 12(9), 1631–1646.

A549 lung cancer cells, Bioorg. Med. Chem., 2006, 14(9), 3218–3222.